

Strain Mediated Magneto-Dielectric & Magneto-resistive Ceramics of $x(\text{Pb}_{0.9}\text{Ti}_{0.1}\text{Fe}_{12}\text{O}_{19})-(1-x)(\text{Pb}_{1-x}\text{Gd}_x\text{TiO}_3)$ where $x =$ **0.50, 0.52, 0.54, 0.56, 0.58 & 0.60**

Jagvir Singh¹, Dr. Sunil Kumar Dwivedi², Dr. Sandeep Sharma³

Submitted:02/05/2024

Revised:16/06/2024

Accepted:25/06/2024

Abstract: Magneto-dielectric & Magneto-resistive Ceramics Composites of Ti^{4+} and Gd^{3+} modified $\text{PbFe}_{12}\text{O}_{19}$ & PbTiO_3 have been prepared using mechanical mixing. The prepared composited system $x(\text{Pb}_{0.9}\text{Ti}_{0.1}\text{Fe}_{12}\text{O}_{19})-(1-x)(\text{Pb}_{1-x}\text{Gd}_x\text{TiO}_3)$ where $x = 0.50, 0.52, 0.54, 0.56, 0.58$ & 0.60 have been reported for Magneto-dielectric & Magneto-resistive response. Polarization vs. Applied Electric field hysteresis endorsed ferroelectric properties whereas Magnetization vs. Applied Magnetic field curve reveals magnetic properties present in prepared composites. Presence of both ferroelectric and magnetic characters concurrently stamped presence of multiferroism in prepared ceramic composites. X-rays diffraction peaks at particular 2θ shows confirmation of presence of structural phases corresponds to structural phase of individual components of ceramic composites. Morphological analysis of prepared composites has been studied from microstructural graphs recorded by scanning electron microscope. S shaped Magnetization vs. magnetic Field hysteresis curves with lesser coercivity reveals ferromagnetic behavior with low magnetic loss. Change in dielectric permittivity, dielectric loss, & resistance directly manifest presence of magneto-electric effect in prepared ceramic composites.

Keywords: Multiferroics, Composites, Magneto-Dielectric, Magneto-Resistance, Dielectric Relaxation.

1. Introduction:

Interest in advanced materials which exhibits next generation properties are current research interest because such materials behaves like back bone of society. Multiferroism results due to concurrently appearance of two or more ferroic order simultaneously in either single or multiple phase materials has gained interest in recent years. Numerous potential uses of multiferroic materials including multiple-state memory elements, novel memory media, transducers, and new functional

sensors etc. possible by electromagnetic effect results from the coupling of magnetic and electric ordering in multiferroic materials made these materials important for various industrial applications. The coupling of such order named as magnetoelectric coupling means tailoring of electric properties by using magnetic field [1-5]. Thus, preparation of a material with strong ferromagnetism and huge ferroelectricity would be revolutionary materials for functionalized materials and current electric devices. In the past, researchers developed conventional perovskite oxides for multiferroic possibilities. In these, BiFeO_3 was a very common example but these perovskite oxides however show modest ferromagnetism along with ferroelectric ordering and single phase. Single phase synthesis of BiFeO_3 was challenge and also gained least interest of researcher and scientist because of Bi_2O_3 because it reduces melting point with which it processed but also exhibits low magnetoelectric coupling. $\text{PbFe}_{12}\text{O}_{19}$ is a very well known as M-type hexaferrites have garnered

¹Research Scholar, Department of Physics, Om Sterling Global University, Hisar

²Associate Professor, Department of Physics, Om Sterling Global University, Hisar

³Associate Professor, HOD Department of Physics, S. R. R. M. Govt College, Jhunjhunu, Rajasthan

Email id: jagvirphy221@osgu.ac.in1;
ksunildwivedi@gmail.com2;
sharma.jjn39@gmail.com3

significant interest due to their unexceptional magnetic and dielectric responses as well as potential for usage in number of individual industrial applications. It has been reported $\text{PbFe}_{12}\text{O}_{19}$ also exhibits ferroelectric properties categorized itself as multiferroic materials [6]. Due to its enormous magneto crystalline anisotropies, high saturation magnetization, and coercivity and ferroelectric polarization as well as dielectric properties, it is used in permanent magnets, plastic magnets, recording medium, and high frequency and microwave components. Due to its multiferroic response, it can also be used in four stage storage applications where (-P, +P, -M & +M) can be used as signal. Here (-P & +P) is ferroelectric polarization and (-M & +M) corresponds to saturation magnetization. Therefore $\text{PbFe}_{12}\text{O}_{19}$ can be considered as one of good candidates for synthesis of multiferroic composites among hexaferrite. We will demonstrate that strong room-temperature ferromagnetism and huge spontaneous polarization of $\text{PbFe}_{12}\text{O}_{19}$ ceramic made it crucial candidate for synthesis of multiferroic composites. On the hand, PbTiO_3 is good ferroelectric perovskites among ferroelectric family due to its maximum dielectric constant (ϵ'), ferroelectric polarization both remnant as well as saturation polarization (P_r & P_s) but highest ferroelectric transition temperature (T^{FE}_{C}) creates major hurdle. It should be assumed that near transition temperature (T^{FE}_{C}), dielectric constant (ϵ') appears maximum. The substitution of rare earth ions at A site of PbTiO_3 decreases ferroelectric transition temperature (T^{FE}_{C}) [7]. In this work, this paper will address simultaneous occurrence of ferromagnetism and ferroelectricity in PFO based composite ceramics. Mishra et al. reports multiferroic behavior in ceramic composites of Pb-M Hexaferrite and PbTiO_3 . The ceramic composites have been synthesized using conventional mechanical mixing approach. Hexaferrite exhibits planar or uniaxial anisotropy and responsible for soft magnetic response. Crystal structure of hexaferrite is hexagonal resemble with magnetoplumbite. Pb-M belongs to family of magnetoplumbite. The structural formation of hexaferrite composed of Sr-O closely packed in in which Fe^{3+} (Five Ions) in octahedral ($\uparrow 12k$, $\uparrow 2a$ and $\downarrow 4f2$) along with tetrahedral ($\downarrow 4f1$) as well as trigonal bipyramidal ($\uparrow 2b$) symmetries [8]. Two crystal block of spinel (s & R) separated. The s spinel block contains $\text{Fe}_{12}\text{O}_{16}$ whereas R block

mainly of PbFeO_3 and belongs to D46h factor group with two formula units per unit cell.

Ajay et al. report multiferroic properties in nanocomposites of PbTiO_3 & SrM hexaferrites. Distortion arises by substitution of Pb^{2+} & Ti^{4+} ions at Sr^{3+} & Fe^{3+} in ($\text{SrFe}_{12}\text{O}_{19}$) lattice studied from broadening in diffraction peaks as increasing PbTiO_3 concentration. Compressive stress identified from asymmetric broadening and peak position shift in Raman spectra in $\text{SrFe}_{12}\text{O}_{19}$ lattice due to PbTiO_3 reveals phonon confinements. Based on electron paramagnetic resonance (EPR) characteristics, influence of PbTiO_3 concentration on spin dynamics and magnetic interactions in these multiferroic nanocomposites has been deduced. The change in voltage with application of magnetic field endorsed magneto-electric coupling and $x = 0.30$ sample exhibits maximum value of ' αME ' and magneto-striction appears in sample when magnetic field on responsible for magneto-electric coupling. Strong dipolar interaction due to multivalent state of Fe appears as results of interstitials substitution of Ti^{4+} at Fe^{3+} ions at octahedral structure as well as strong broad resonance signal. The magnetic sensor application will make use of these nanocomposites [9]. $\text{PbFe}_{12}\text{O}_{19}$ commonly written as (PFO) exhibits a strong ferromagnetic response whilst PbTiO_3 cited as (PTO) results for ferroelectric order because it most commonly used ferroelectric perovskite among its family. The amalgamation of these two component results in a multiferroic system. X-ray diffraction study has been revealed that diffraction peak at $2\theta \sim 32.3$ & 34.3 confirmed hexaferrite structural phase of $\text{PbFe}_{12}\text{O}_{19}$ whereas diffraction peaks corresponds to $2\theta \sim 31.6$ & 32.3 reveals presence of ferroelectric phase PbTiO_3 and evidence for successful synthesis of ceramic composites with minimal interface interaction. Micrographs recorded using scanning electron microscope reveals equilibrated distribution of PFO and PTO grains. Polarization vs. Electric field & Magnetization vs. Magnetic field hysteresis appears in ceramic composites stamped for presence of multiferroism in prepared composites. Remnant polarization values (P_r) of $8.84 \mu\text{C}/\text{cm}^2$, $4.65 \mu\text{C}/\text{cm}^2$, $2.48 \mu\text{C}/\text{cm}^2$, and $0.52 \mu\text{C}/\text{cm}^2$ in prepared ceramic composites shows PbTiO_3 is responsible for such large polarization in prepared composites samples whereas high magnetic moment results due to Pb-M hexaferrite content in composite composition. Magnetic hysteresis

reveals that remnant magnetization (M_r) tailored from 0.00029 emu/g to 27.74 emu/g as content of Pb-M ferrite increases in composites by wt%. The least value of magnetization in PbTiO_3 rich composites composition results due to either nonmagnetic PbTiO_3 phase or domain wall pinning effect. This highlights a significant area of inquiry for composite ceramics possessing multiferroic characteristics. Typical magnetic hysteresis loops show substantially varying magnetization and coercive forces with continuous changing of content of PbMhexaferrite [10].

In this paper, composites of Gd^{3+} modified PbTiO_3 and Ti^{4+} modified $\text{PbFe}_{12}\text{O}_{19}$ in stoichiometric proportion of $x(\text{Pb}_{0.9}\text{Ti}_{0.1}\text{Fe}_{12}\text{O}_{19}) - 1-x(\text{Pb}_{0.75}\text{Gd}_{0.25}\text{TiO}_3)$ where $x = 0.50, 0.52, 0.54, 0.56, 0.58 \text{ \& } 0.60$ have been prepared to explore effect of magnetic, dielectric and magneto-dielectric traits. Insite of above, structural, microstructural and elemental confirmation has also be studied in details. Elemental mapping has also be elaborated to study extent of distribution of various elements.

2. Experimental:

Using mechanical mixing technique, ceramic composites of $x(\text{Pb}_{0.9}\text{Ti}_{0.1}\text{Fe}_{12}\text{O}_{19}) - 1-x(\text{Pb}_{1-x}\text{Gd}_x\text{TiO}_3)$ where $x = 0.50, 0.52, 0.54, 0.56, 0.58 \text{ \& } 0.60$ have been created. In this case, individual $\text{Pb}_{0.9}\text{Ti}_{0.1}\text{Fe}_{12}\text{O}_{19}$ has been synthesized by a wet chemical technique, while $\text{Pb}_{1-x}\text{Gd}_x\text{TiO}_3$ has been synthesized individually using solid state reaction approach. The required oxides have been obtained from Sigma Aldrich. The composites of above mentioned ceramics (Ferroelectric & Ferromagnetic) in mention stoichiometric proportion have been synthesized using mechanical mixing route using high energy planetary ball milling machine for 24 hours. The mixed powder taken out from Teflon jar used in high energy planetary ball milling machine and left for drying. The dried powder mixed with polymer binder which most commonly used named as polyvinyl alcohol and pressed into pellets in circular shapes like discs using high pressure dye and hydyluric press. In order to investigate presence of both structural phase, X-ray diffraction has been carried. The high intensity diffraction peaks correspond to 2θ of ferrite and perovskite endorsed for presence of both (Ferroelectric and Ferromagnetic) phases. Porosity, grain growth of prepared ceramic composites has been analyzed from scanning

electron micrographs whereas energy dispersive spectroscopy validated elements mentioned above. Elemental mapping provides information about distribution of various metal ions in ceramic matrix. A lab-made setup based on the Archimedes principle was used to assess density of the sintered pellet. Vibrating sample magnetometer has been used to examine shape of M vs. H hysteresis which provides information on magnetic ordering that is present at room temperature. Using an impedance analyzer, ϵ' , ϵ'' & σ_{ac} vs. frequency have been obtained to illustrate the impact of Ti modified $\text{PbFe}_{12}\text{O}_{19}$ on dielectric behavior of Gd modified PbTiO_3 in form of composites. The ϵ' , ϵ'' & σ_{ac} vs. frequency as well as change resistance vs Frequency with magnetic field endorsed of presence of magnetodielectric response in prepared ceramic composites.

3. Result & Discussion

Room Temperature diffraction data of $x(\text{Pb}_{0.9}\text{Ti}_{0.1}\text{Fe}_{12}\text{O}_{19}) - 1-x(\text{Pb}_{1-x}\text{Gd}_x\text{TiO}_3)$ where $x = 0.50, 0.52, 0.54, 0.56, 0.58 \text{ \& } 0.60$ magneto-dielectric composites have been shown in Figure 1. The sharp edged high intensity diffraction peaks reveals crystalline behavior of prepared composite samples. To study crystal phases, present in composite samples, diffraction data 2θ vs. Intensity (a.u.) have been studied using reported diffraction data of related crystal structures or JCPDS cards which explore particular crystal structures properties (d-spacing, Lattice parameters etc.) according to structural phase. All diffraction peaks analyzed using JCPDS cards of tetragonal phases of PbTiO_3 and of hexagonal phases of M-type ferrite and indexed according to their crystal plane. All diffraction peaks have been indexed according to diffraction peaks given in JCPDS card no. 78-0299 which represents tetragonal structural phase (Space Group No. 99 and symbol P 4 mm) and 79-1411 of hexagonal structural phase of $\text{SrFe}_{12}\text{O}_{19}$ considered as M-type hexaferrite (Space Group $\text{P6}_3/\text{mmc}$ No. 194). No diffraction peak left unindexed means both structural phases in mentioned space group present in ceramic composites. The diffraction peaks particularly appears at $2\theta \sim 32.41 \text{ \& } 34.23$ considered as direct evidence of presence of hexagonal structural phase of M-type hexaferrite ($\text{PbFe}_{12}\text{O}_{19}$) whereas diffraction peaks corresponds to $2\theta \sim 22.7 \text{ \& } 31.7$ reveals presence of ferroelectric phase PbTiO_3 . Appearance of these diffraction peaks

The strain and dislocation density has been calculated using formula and tabulated given as Eq 3 & 4 in Table 2 given below

$$\varepsilon = \beta \cos \theta / \dots (\text{Eq. 3})$$

$$\delta = 1 / \text{Average Crystallite Size (D)} \dots (\text{Eq. 4})$$

Table 2: Crystallographic Signatures (Strain (ε), Dislocation Density (δ) vs. Composition (x) of $1-x\{\text{Pb}_{0.74}\text{Pr}_{0.25}\text{O}_3\}-x\{\text{Pb}_{0.9}\text{Ti}_{0.1}\text{Fe}_{12}\text{O}_{19}\}$ Magneto-Dielectric Ceramic Composites where $x = 0.50, 0.52, 0.54, 0.56, 0.58 \text{ \& } 0.60$

Composition↓ Crystal Phase→	Hexagonal		Tetragonal [13]	
	ε	$\delta \text{ (m}^{-3}\text{)}$	ε	$\delta \text{ (m}^{-3}\text{)}$
$x = 0.50$	0.00093	0.00032	0.0014	0.00030
$x = 0.60$	0.00064	0.00071	0.00062	0.0018

The table 2 clearly indicates that in composites having same weight proportionate in stoichiometry of composites, larger strain induces because of large difference in size of unit cell volume (Hexagonal & Tetragonal) and corresponds dislocation density.

Surface morphology such as extent of porosity, grain growth and grain size has studied from micrographs collected using FESEM. The micrographs of prepared magneto-dielectric ceramic composites of $x(\text{Pb}_{0.9}\text{Ti}_{0.1}\text{Fe}_{12}\text{O}_{19})-1-x(\text{Pb}_{1-x}\text{Gd}_x\text{TiO}_3)$ where $x = 0.50, 0.52, 0.54, 0.56, 0.58$ & 0.60 have been shown in figure 2. Micrographs

exhibit grains of different size, non-uniformly distributed and of hexagonal, circular and plate like shapes clearly visualized. The hexagonal and plate like grains corresponds to hexagonal structure whereas circular grains represent ferroelectric perovskite phase. The hexagonal; shape of the prepared samples causes a decrease of grain boundary and surface energy. Micrographs also point towards agglomeration of smaller grains due to magnetic interaction between the individual grains of the prepared samples. The extent of cross-linked grains shows grain growth.

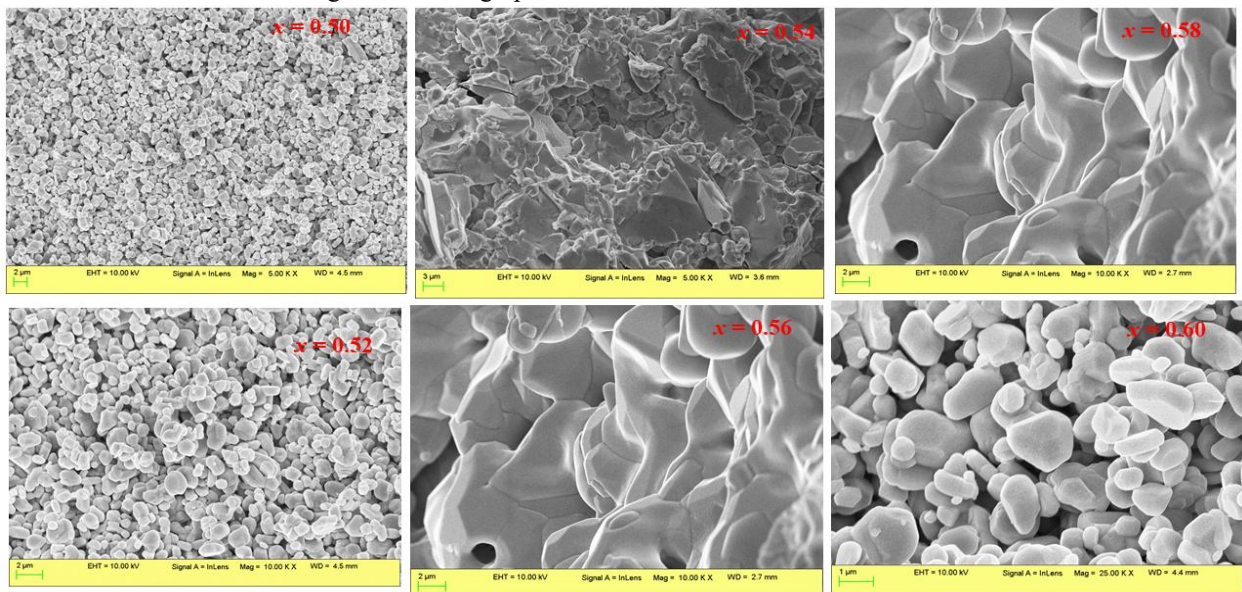


Figure 2: Morphological Representation at Micron level of $x(\text{Pb}_{0.9}\text{Ti}_{0.1}\text{Fe}_{12}\text{O}_{19})-1-x(\text{Pb}_{1-x}\text{Gd}_x\text{TiO}_3)$ magneto-dielectric composites

To further confirms successful synthesis of ceramic composites, elemental confirmation has been carried out using energy dispersive spectroscopy. The electron micrograph in selected area from which x-rays generated has been shown in figure 3

of $x = 0.60$. The peaks corresponding to their binding energy confirms appearance of elements mentioned in stoichiometric proportion manifest for successful synthesis of reported ceramic composites.

Spectrum processing :
Peak possibly omitted : 3.715 keV
Processing option : All elements analyzed (Normalised)
Number of iterations = 4
Standard :
O SiO2 1-Jun-1999 12:00 AM
Ti Ti 1-Jun-1999 12:00 AM
Fe Fe 1-Jun-1999 12:00 AM
Gd GdF3 1-Jun-1999 12:00 AM
Pb PbF2 1-Jun-1999 12:00 AM

Element	Weight%	Atomic%
O K	72.47	97.13
Ti K	-0.01	0.00
Fe K	0.07	0.03
Gd L	0.00	0.00
Pb M	27.46	2.84
Totals	100.00	

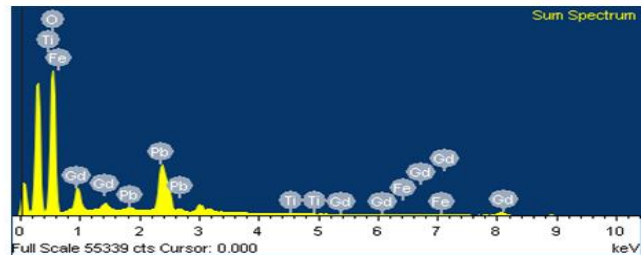
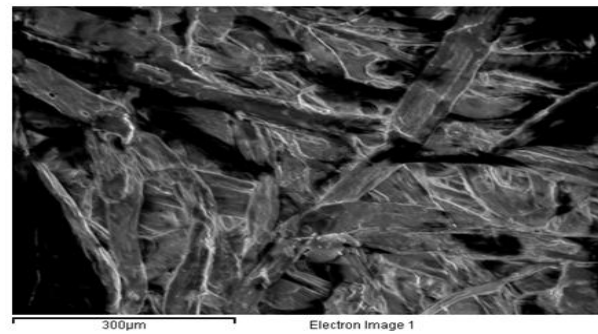


Figure 3: Morphological Representation at Micron level of $x(\text{Pb}_{0.9}\text{Ti}_{0.1}\text{Fe}_{12}\text{O}_{19})$ - $1-x(\text{Pb}_{1-x}\text{Gd}_x\text{TiO}_3)$ magneto-dielectric composites

Distribution of elemental in as mentioned in stoichiometric proportion have been confirmed by mapping of elements in selected area in given electron micrograph and shown in figure 4 of $x =$

0.60. Different colours have been assigned metal ion have been assigned different colour. The micro-graph with mixed colours shows uniform distribution of different-different metal ions.

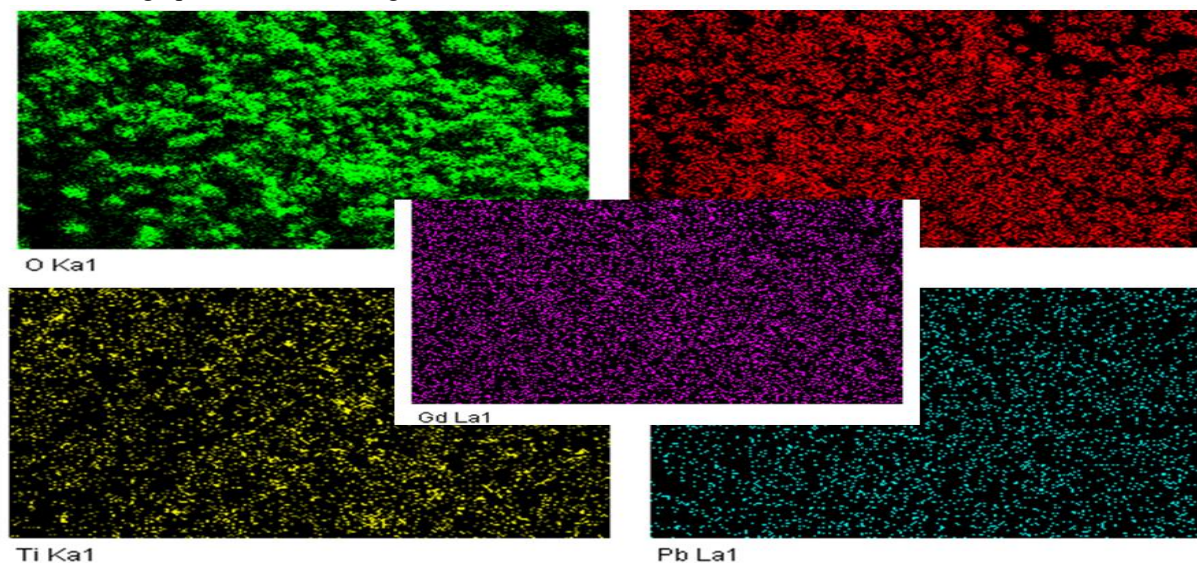


Figure 4: Distribution of $x(\text{Pb}_{0.9}\text{Ti}_{0.1}\text{Fe}_{12}\text{O}_{19})$ - $1-x(\text{Pb}_{1-x}\text{Gd}_x\text{TiO}_3)$ magneto-dielectric composites

Magnetic properties at room temperature of $x(\text{Pb}_{0.9}\text{Ti}_{0.1}\text{Fe}_{12}\text{O}_{19})$ - $1-x(\text{Pb}_{1-x}\text{Gd}_x\text{TiO}_3)$ where $x = 0.50, 0.52, 0.54, 0.56, 0.58$ & 0.60 magneto-dielectric composites have been measured at using vibrating sample magnetometer shown in figure 5. Magnetic Moment vs. Magnetic Field hysteresis shown in figure 3. The saturation magnetization as well as remnant magnetization increases as content of Ti^{4+} modified $\text{PbFe}_{12}\text{O}_{19}$ increases. Magnetic moment in magneto-dielectric composites may

result due to up and down spin of Fe^{3+} in sub lattice at octahedral site. 24 Fe^{3+} ions at tetrahedral sub lattice. The antiparallel and parallel spins of Fe^{3+} coupled with each other results in super exchange interaction of Fe^{3+} -O- Fe^{3+} . The value of saturation magnetization (M_s), Remnant Magnetization (M_r) and coercivity (H_c) have been tabulated in table 1. It has been clearly seen from table that remnant Magnetization (M_r) increases from 2.35 emu/g for $x = 0.50$ to 7.61 emu/g for $x = 0.60$. The saturation

(M_r) also increases from 18.95 emu/g to 36.64 emu/g. The small value of coercivity (H_c) made these material suitable candidates for transformer

manufacturing because low coercivity (H_c) arrowed towards easy magnetization without magnetic loss.

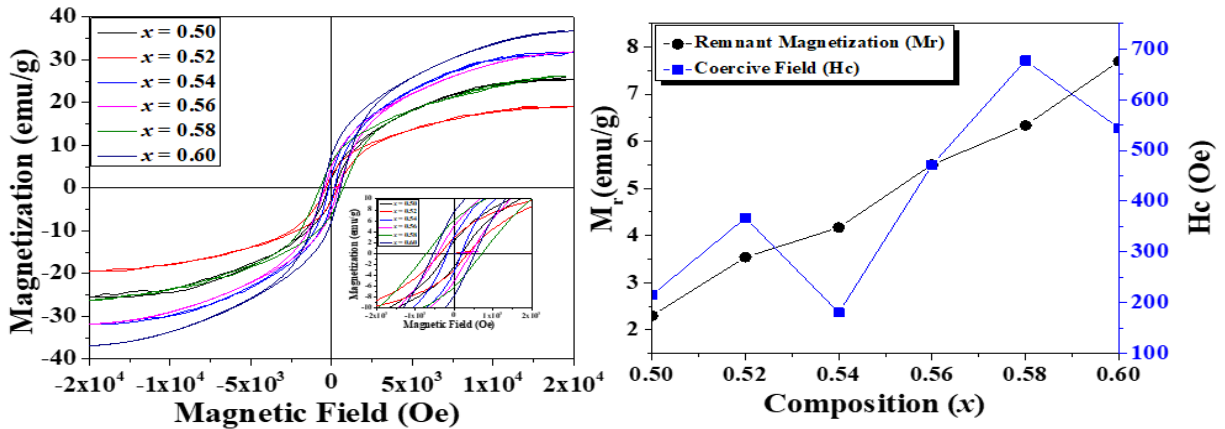


Figure 5: Magnetic Field vs. Magnetization curve and Magnetic properties of $x(\text{Pb}_{0.9}\text{Ti}_{0.1}\text{Fe}_{12}\text{O}_{19})-(1-x)(\text{Pb}_{1-x}\text{Gd}_x\text{TiO}_3)$ magneto-dielectric composites

Room Temperature Dielectric properties (ϵ' & $\tan\delta$ vs. frequency) of $x(\text{Pb}_{0.9}\text{Ti}_{0.1}\text{Fe}_{12}\text{O}_{19})-(1-x)(\text{Pb}_{1-x}\text{Gd}_x\text{TiO}_3)$ magneto-dielectric composites have been carried to explore effect of Ti^{4+} modified $\text{PbFe}_{12}\text{O}_{19}$ on Pb^{2+} partially substituted with Nd^{3+} in (PbTiO_3) in the frequency range varying from 0.1kHz-1MHz. ϵ' and $\tan\delta$ vs. frequency has been shown in figure 6(a) and 6(b) respectively. The graphs clearly manifest that as frequency increases, both real part of dielectric permittivity and $\tan\delta$ decreases and after a particular both become constant. Such type of behavior leads to contribution as well as frequency dependence of various polarizations named as dipolar, ionic, electronic and

interfacial polarizations. It has been assumed that in low frequency regime, all polarization contributes maximum and as frequency increases, their contribution starts diminishing and become almost negligible in higher frequency range results in constant value of ϵ' and $\tan\delta$. Such kind of response of polarization towards frequency can be explained using dipole relaxation phenomenon [14-17]. The Cole-Cole relaxation model (modified form of Debye relaxation model) has been used to explain the relaxation phenomenon. According to this model, the ϵ' and ϵ'' vary with frequency as:

$$\epsilon'(\omega) = \epsilon_{\infty} + (\epsilon_s - \epsilon_{\infty}) \frac{1 + (\omega\tau_0)^{1-\alpha} \sin \frac{1}{2} \alpha \pi}{1 + 2(\omega\tau_0)^{1-\alpha} \sin \frac{1}{2} \alpha \pi + (\omega\tau_0)^{2(1-\alpha)}}$$

$$\epsilon''(\omega) = (\epsilon_s - \epsilon_{\infty}) \frac{(\omega\tau_0)^{1-\alpha} \cos \frac{1}{2} \alpha \pi}{1 + 2(\omega\tau_0)^{1-\alpha} \sin \frac{1}{2} \alpha \pi + (\omega\tau_0)^{2(1-\alpha)}}$$

where ϵ_{∞} = dielectric constant measured at high frequency, ϵ_s = dielectric constant measured at low frequency, $\omega = 2\pi f$ the angular frequency of applied field and τ = characteristics relaxation time of the medium. The exponent parameter α usually

varies between 0 and 1, and it describes the shape of spectral curves. It may be noted that for $\alpha = 0$, the Cole-Cole model reduces to the Debye model. [23].

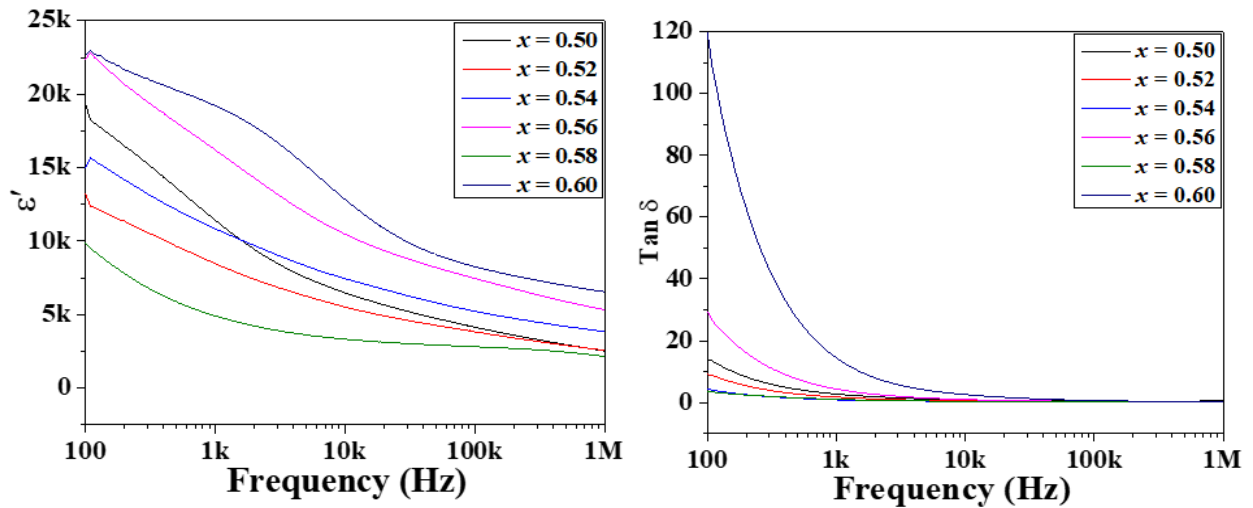


Figure 6: (a) ϵ' vs. frequency (b) $\tan\delta$ vs. frequency of $x(\text{Pb}_{0.9}\text{Ti}_{0.1}\text{Fe}_{12}\text{O}_{19})-(1-x)(\text{Pb}_{1-x}\text{Gd}_x\text{TiO}_3)$ magneto-dielectric composites

Figure 6 shows the frequency dependence of electrical conductivity of $x(\text{Pb}_{0.9}\text{Ti}_{0.1}\text{Fe}_{12}\text{O}_{19})-(1-x)(\text{Pb}_{1-x}\text{Gd}_x\text{TiO}_3)$ magneto-dielectric composites. The ac conductivity is calculated from the measured dielectric data using the relation: $\sigma_{ac} = 2\pi f \epsilon' \epsilon_0 \tan\delta$ [18], where the parameters have their usual meaning. It can be observed that the ac conductivity increases with increasing frequency for all compositions. It is further clear from the figure that the conductivity shows two distinct regimes within the measured frequency limit, (i) the plateau and (ii) the dispersion region. The plateau region corresponds to low frequency region. In this region, the conductivity has been

found to be independent of frequency. The dispersion region corresponds to high frequency region. In this region, conductivity increases with increase in frequency. In fact, the plateau region corresponds to dc conductivity (σ_{dc}) and dispersion region corresponds to ac conductivity (σ_{ac}). The frequency dependence of ac conductivity in ceramics is generally analyzed by Jonscher's power law [18]: $\sigma_{ac} = \sigma_{dc} + A \omega^n$, where "A" is the dispersion parameter representing the strength of polarizability and "n" is the dimensionless frequency exponent representing the interaction between mobile ions with the lattice around them [19].

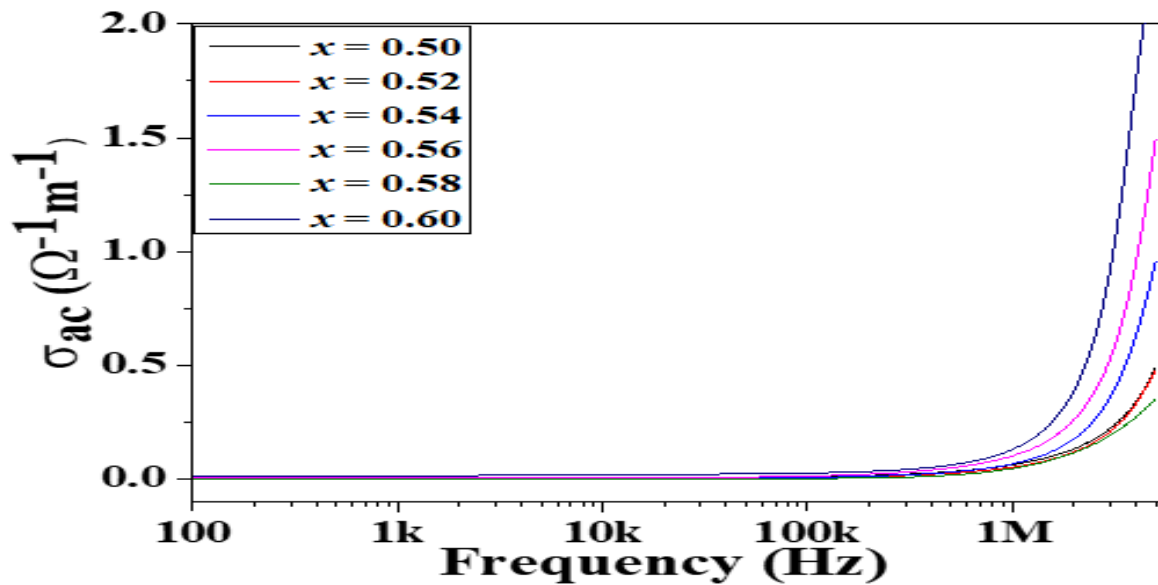


Figure 7: σ_{ac} vs. frequency of $x(\text{Pb}_{0.9}\text{Ti}_{0.1}\text{Fe}_{12}\text{O}_{19})-(1-x)(\text{Pb}_{1-x}\text{Gd}_x\text{TiO}_3)$ magneto-dielectric composites

Influence of magnetic field has been investigated from change in dielectric properties such dielectric

permittivity (ϵ'), dielectric loss (D) vs. frequency (Hz). Such variation of dielectric properties with

magnetic field (H_{0e}) has been pronounced as magneto-dielectric response (MDR) and be calculated given below. Such magnetically

$$MD = \frac{\epsilon(H) - \epsilon(0)}{\epsilon(0)} \times 100 \%$$

Or

$$ML = \frac{D(H) - D(0)}{D(0)} \times 100 \%$$

where; MD is magnetodielectric coefficient, $\epsilon(H)$ and $\epsilon(0)$ are their standard means termed as real part of dielectric constant at strength of magnetic field values H_{0e} and H_0 , respectively, D pronounced as dielectric loss at the same frequency

influenced dielectric is an indirect evidence for magneto-electric coupling. MD (in terms of percentage) has been calculated using Eq. 3[21]:

and ML abbreviated as magneto-loss . It has been clearly observed from figure that change of MD response with magnetic field at 20 kHz. The values of MD and ML have been tabulated in Table II.

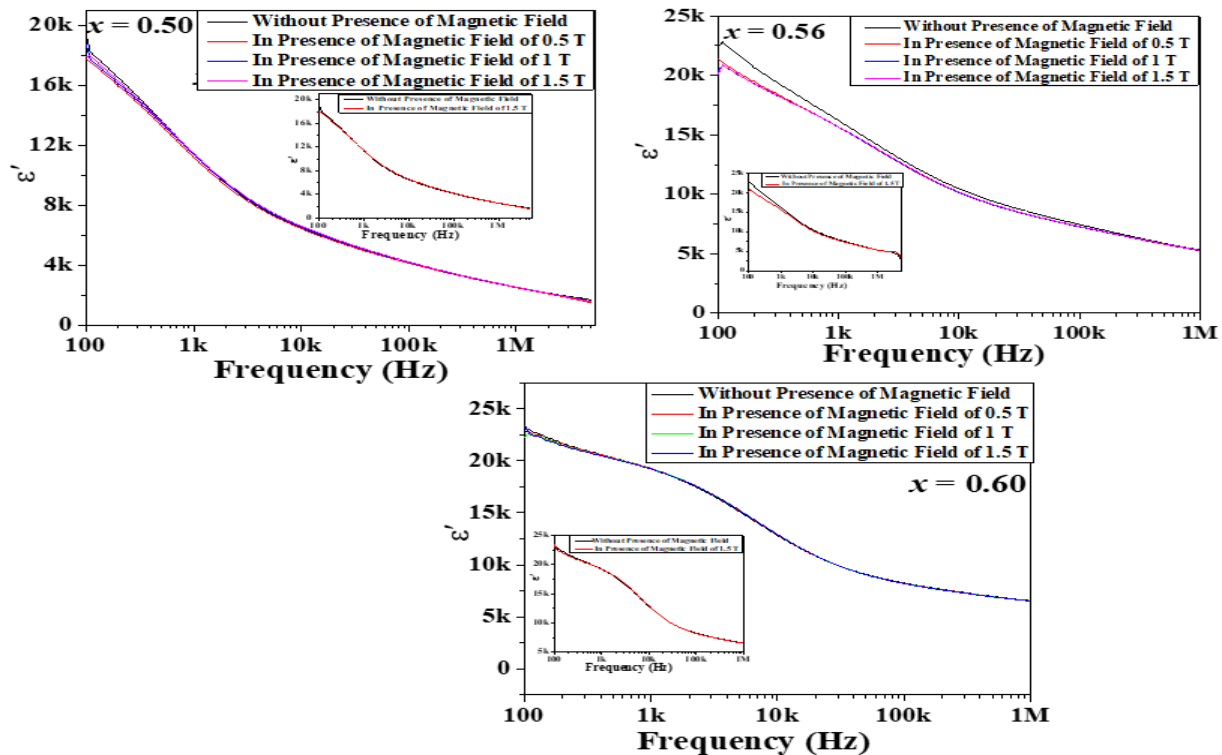


Figure 8: Magneto-Dielectric Response (Change in Dielectric Constant with Magnetic Field) of $x(\text{Pb}_{0.9}\text{Ti}_{0.1}\text{Fe}_{12}\text{O}_{19})-(1-x)(\text{Pb}_{1-x}\text{Gd}_x\text{TiO}_3)$ magneto-dielectric composites

The values of magneto-dielectric response or magneto-loss reveals that with increase in magnetic field, MD& ML increases in negative direction and gets saturated at higher values of magnetic field. This indicates the presence of negative coupling in the composites. It can be seen that the values of MD increases from $x = 0.5$ to 0.56 and reaches a

maximum, which is relatively higher comparing to recently reported KNN based multiferroic composites, indicating strong magnetoelectric coupling effect [21-22]. The magnetodielectric response of composite sample for $x = 0.6$ at certain frequencies individually shown in figure.

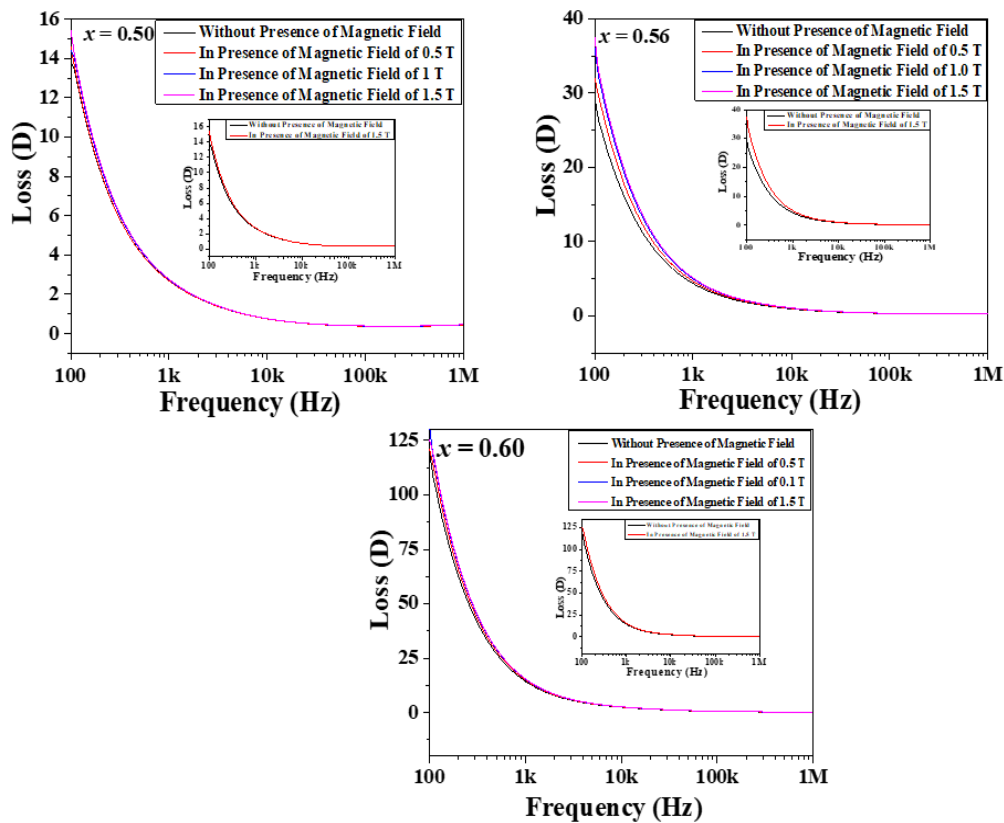


Figure 9: Magneto-Dielectric Response (Change in Dielectric Loss with Magnetic Field) of $x(\text{Pb}_{0.9}\text{Ti}_{0.1}\text{Fe}_{12}\text{O}_{19})$ - $1-x(\text{Pb}_{1-x}\text{Gd}_x\text{TiO}_3)$ magneto-dielectric composites

To further confirm effect of magnetic field on electric properties, resistance (Ω) vs. Frequency profile in presence of magnetic field has been collected and effect of magnetic on resistance has

been calculated using formula given below and shown in figure

$$MR = \frac{R(H) - R(0)}{R(0)} \times 100\%$$

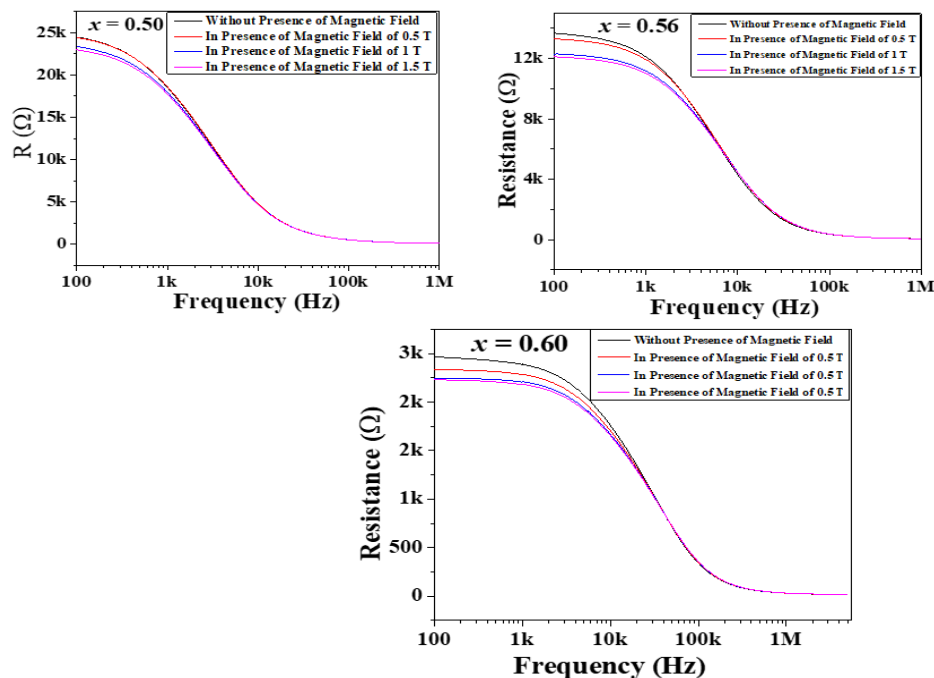


Figure 10: Magneto-Electric Response (Change in Resistance with Magnetic Field) of $x(\text{Pb}_{0.9}\text{Ti}_{0.1}\text{Fe}_{12}\text{O}_{19})$ - $1-x(\text{Pb}_{1-x}\text{Gd}_x\text{TiO}_3)$ magneto-dielectric composites

4. Conclusion

$x(\text{Pb}_{0.9}\text{Ti}_{0.1}\text{Fe}_{12}\text{O}_{19})$ - $1-x(\text{Pb}_{1-x}\text{Gd}_x\text{TiO}_3)$ magneto-dielectric composites have been successfully synthesized. Crystal structures analysis of prepared magneto-dielectric ceramic composites found to be perovskite tetragonal and hexagonal of magnetic ferrite without any secondary phase. Magnetic hysteresis clearly reveals that with change of ferrite content in composites concentration, ferromagnetic behavior dominates over ferroelectric response result in increase in dielectric loss as well as conductivity. The variation in dielectric constant with magnetic field confirms magnetodielectric effect which is attributed due to strain mediated stress with applied magnetic field in composites. The maximum value of magneto dielectric response has been found to indicating negative magnetodielectric effect.

5. References

- [1] Guolong Tann, Xiuna Chen, Structure and multiferroic properties of barium hexaferrite ceramics, *Journal of Magnetism and Magnetic Materials* 327 (2013) 87–90
- [2] Meera Rawat and K L Yadav, Electrical, magnetic and magnetodielectric properties in ferrite-ferroelectric particulate composites, *IOP Publishing, Smart Materials and Structures, Smart Mater. Struct.* 24 (2015) 045041 (11pp) doi:10.1088/0964-1726/24/4/045041
- [3] Ayesha Khalid, Ghulam M. Mustafa, ShahzadNaseem, ShahidAtiq, Sm-mediated dielectric characteristics and tunable magneto-electric coefficient of $0.5\text{Bi}_{1-x}\text{Sm}_x\text{Fe}_{0.95}\text{Mn}_{0.05}\text{O}_3$ - 0.5PbTiO_3 composites, *Ceramics International* 45 (2019) 7690-7695
- [4] KanchanBala, R.K. Kotnalab, N.S. Negi, Magnetically tunable dielectric, impedance and magnetoelectric response in $\text{MnFe}_2\text{O}_4/(\text{Pb}_{1-x}\text{Sr}_x)\text{TiO}_3$ composites thin films, *Journal of Magnetism and Magnetic Material*, 424 (2017), 256-266
- [5] Himani Joshi, A. Ruban Kumar, Investigations and Correlations of Structural, Magnetic, and Dielectric Properties of M-Type Barium Hexaferrite ($\text{BaFe}_{12}\text{O}_{19}$) for Hard Magnet Applications, *Journal of Superconductivity and Novel Magnetism* (2022) 35:2435–2451
- [6] Muhammad Zahid, Hasan M. Khan M. A. Assiri, Muhammad I., Saeed Ahmad Buzdar Structural, Morphology, Dielectric, and Magnetic Properties of $\text{Pb}_{1-x}\text{Cr}_x\text{Fe}_{12}\text{O}_{19}$ M-type Hexaferrite, *Materials Science and Engineering B*, 280, (2022), 115707
- [7] Akshay Kumar, Kanchan Khanna, Tiku Ram, Sunil K. Dwivedi and Sunil Kumar, Correlation between Sintering Temperature and Structural, Ferroelectric Properties of $\text{Pb}_{0.75}\text{Nd}_{0.25}\text{TiO}_3$ Ceramics, *Material Today Proceedings*, 65, 1(2022) 322-326,
- [8] Hexaferrite Ashraf M. Semaida, Moustafa A. Darwish, Sergei V. Trukhanov, MohamedM.Salem3, DiZhou4, Alex V. Trukhanov, Vladimir P. Menushenkov, Tatiana I. Zubar, and Alexander G.Savchenko Impact of Nd^{3+} Substitutions on the Structure and Magnetic Properties of Nanostructured $\text{SrFe}_{12}\text{O}_{19}$
- [9] Ajay S., Balwinder Kaur, Manju A., Vishal S., Effect of PbTiO_3 concentration on structural, paramagnetic resonance and magnetoelectric properties of PbTiO_3 : $\text{SrFe}_{12}\text{O}_{19}$ multiferroic nanocomposites, *Materials Chemistry and Physics*, 258(2021) 123849
- [10] Adebayo, M. Deepfakes and Data Privacy: Navigating The Risks in the Age of AI. NDPC–, 106.
- [11] Debesh D. Mishra, Daniel M. Tewelde, Min Wang, Guolong Tan, Multiferroic properties of $\text{PbFe}_{12}\text{O}_{19}$ - PbTiO_3 composite ceramics, *Journal of Materials Science: Materials in Electronics* <https://doi.org/10.1007/s10854-019-01426-6a>
- [12] Gurdev Preet Singh, Jasvir Singh, Khalid Mijasam Batoo, Ahmed Ahmed Ibrahim, Om Prakash, Amritpal Singh Nindrayog, K. J. Singh Experimental and DFT + U Investigations of the $\text{Cu}_{1-x}\text{Cd}_x\text{O}$ Nanoparticles Synthesized for Photocatalytic Degradation of Organic Pollutants: Environmental Application, *Water Air Soil Pollut* (2024) 235:117
- [13] Rajnish, Sunita Dahiya, Sunil Kumar2, and Naveen Kumar, Magnetic, Photoluminescence and Dielectric response in $\text{CuO-Co}_2\text{O}_3$ composites, *J Mater Sci: Mater Electron* (2024) 35:1312
- [14] Himani Joshi, A. Ruban Kumar, Investigations and Correlations of Structural, Magnetic, and Dielectric Properties of M-Type Barium

- Hexaferrite ($\text{BaFe}_{12}\text{O}_{19}$) for Hard Magnet Applications, *Journal of Superconductivity and Novel Magnetism* (2022) 35:2435–2451 <https://doi.org/10.1007/s10948-022-06203-x>
- [15] Kumar M, Yadav KL. *J. Phys.: Condens. Matter*. 2002;19:242202.
- [16] Cole KS, Robert H. Dispersion and Absorption in Dielectrics:- Alternating Current Characteristics. *Journal of Chemical Physics*. 1941;9:341–351.
- [17] Havriliak S, Negami S. A complex plane representation of dielectric and mechanical relaxation processes in some polymers. *Polymer*. 1967;8:161-210. DOI: 10.1016/0032-3861(1967)90021-3.
- [18] Prakash V, Choudhary SN, Sinha TP. Dielectric relaxation in complex perovskite oxide $\text{BaCo}_{1/2}\text{W}_{1/2}\text{O}_3$. *Physica B*. 2008; 403:103–108.
- [19] Jonscher AK. The Universal dielectric response. *Nature*. 1977; 267:673-679.
- [20] Pradhan DK, Behera B, Das PR. Studies of dielectric and electrical properties of a new type of complex tungsten bronze electroceramics. *J. Mater. Sci. Mater. Electron*. 2012; 23:779.
- [21] Dyre JC, Schroder TB. Ac hopping conduction at extreme disorder takes place on the percolating cluster. *PRL*. 2008; 101:025901.
- [22] V.R. Palkar, D.C. Kundaliya, S.K. Malik and S. Bhattacharya, Magnetoelectricity at room temperature in $\text{Bi}_{0.9-x}\text{Tb}_x\text{La}_{0.1}\text{FeO}_3$ system, *Phys. Rev. B*. 69 (2004)212102-3.
- [23] M. Kumar and K.L. Yadav, Study of dielectric, magnetic, ferroelectric and Magnetoelectric properties in the $\text{PbMn}_x\text{Ti}_{1-x}\text{O}_3$ system at room temperature, *J. Phys: Condens. Mater* 19 (2007) 242202 (1-7 pages)